◆ Human Brain Mapping 36:3289–3302 (2015) ◆

Independent Component Analysis of Functional Networks for Response Inhibition: Inter-Subject Variation in Stop Signal Reaction Time

Sheng Zhang,[1]* Shang-Jui Tsai,[2] Sien Hu,[1] Jiansong Xu,[1] Herta H. Chao,[3,4] Vince D. Calhoun,[1,5,6] and Chiang-Shan R. Li[1,7,8]*

[1]*Department of Psychiatry, Yale University, New Haven, Connecticut*
[2]*Department of Medicine, National Yang-Ming University, Taipei, Taiwan*
[3]*Department of Internal Medicine, Yale University, New Haven, Connecticut*
[4]*Medical Service, VA Connecticut Health Care System, West Haven, Connecticut*
[5]*The Mind Research Network, Albuquerque, New Mexico*
[6]*Department of Electrical and Computer Engineering, The University of New Mexico, Albuquerque, New Mexico*
[7]*Department of Neurobiology, Yale University, New Haven, Connecticut*
[8]*Interdepartmental Neuroscience Program, Yale University, New Haven, Connecticut*

Abstract: Cognitive control is a critical executive function. Many studies have combined general linear modeling and the stop signal task (SST) to delineate the component processes of cognitive control. For instance, by contrasting stop success (SS) and stop error (SE) trials in the SST, investigators examined regional responses to stop signal inhibition. In contrast to this parameterized approach, independent component analysis (ICA) elucidates brain networks subserving cognitive control. In our earlier work of 59 adults performing the SST during fMRI, we characterized six independent components (ICs). However, none of these ICs correlated with stop signal performance, raising questions about their behavioral validity. Here, in a larger sample ($n = 100$), we identified and explored 23 ICs for correlation with the stop signal reaction time (SSRT), a measure of the efficiency of response inhibition. At a corrected threshold ($P < 0.0005$), a paracentral lobule-midcingulate network and a left inferior parietal-supplementary motor-somatomotor network showed a positive correlation between SE beta weight and SSRT. In contrast, a midline cerebellum–thalamus–pallidum network showed a negative correlation between SE beta weight and SSRT. These findings suggest that motor preparation and execution prolongs the SSRT, likely via an interaction between the go and stop processes as suggested by the race model. Behaviorally, consistent with this hypothesis, the difference in G and SE reaction times is positively correlated with SSRT across subjects. These new results highlight the importance of cogni-

Additional Supporting Information may be found in the online version of this article.

Contract grant sponsor: NIH; Contract grant number: DA023248; AA021449; P20GM103472; Contract grant sponsor: NSF; Contract grant number: BCS1309260

*Correspondence to: Dr. Sheng Zhang, Connecticut Mental Health Center S103, 34 Park Street, New Haven CT 06519. E-mail: sheng.zhang@yale.edu or Dr. C.-S. Ray Li, Connecticut Mental Health Center S112, 34 Park Street, New Haven CT 06519. E-mail: chiang-shan.li@yale.edu

Received for publication 16 October 2014; Revised 6 March 2015; Accepted 6 April 2015.

DOI: 10.1002/hbm.22819

Published online 18 June 2015 in Wiley Online Library (wileyonlinelibrary.com).

tive motor regions in response inhibition and support the utility of ICA in uncovering functional networks for cognitive control in the SST. *Hum Brain Mapp 36:3289–3302, 2015.*

Key words: fMRI; neuroimaging; stop signal; nogo; inhibitory control; neural network; ICA

INTRODUCTION

The neural bases of cognitive control have long been a focus of research in cognitive neuroscience. Many behavioral tasks are used to examine regional brain activations to the component processes of cognitive control [Egner, 2008]. For instance, in a stop signal task (SST), participants override a prepotent motor response, monitor error, and adjust the speed of response after encountering an error. On the basis of linear models, our previous functional magnetic resonance imaging (fMRI) studies of the SST examined regional brain activations involved in these component processes [Li et al., 2006, 2008a,b,c]. By contrasting stop success (SS) and stop error (SE) trials, we observed greater activation in the anterior pre-supplementary motor area (SMA) in association with faster stop signal reaction time (SSRT) and attributed these regional responses to motor inhibition [Chao et al., 2009; Duann et al., 2009; Li et al., 2006]. These studies complement a large body of electrophysiological and imaging research that employed event contrasts to identify the neural correlates of the component processes of cognitive control [Huster et al., 2013; Kok et al., 2004; Swann et al., 2012].

However, the approach of "cognitive subtraction" is known to involve methodological issues [Friston et al., 1996; Logothetis, 2008]. That is, by contrasting two β's from the generalized linear model (GLM) and labeling the difference as specific to a psychological construct, one would have to assume that all other constructs are equally represented in the two β's, an assumption that all too often is not valid [Friston et al., 1996]. For instance, in an earlier work, we examined how activations during errors and post-error slowing (PES) may be related and were puzzled by a lack of correlation between any regional error responses and ventrolateral prefrontal cortical (vlPFC) activation during PES [Li et al., 2008a]. In a subsequent work, we employed Granger causality mapping to identify voxels that Granger caused vlPFC during the SST [Ide and Li, 2011]. The analyses revealed a cortical thalamic cerebellar circuit that precedes vlPFC activity. In particular, we observed that, while the β's of these regions during error detection were correlated to vlPFC activity during PES, the mean values were not substantially different from zero and thus eluded the detection by GLM. This study exemplified the limitation of "cognitive subtraction" in identifying the neural bases of a psychological construct.

Independent component analysis (ICA) represents an alternative approach to identify networks of brain regions in response to events of interest. As a data driven method, ICA uncovers hidden factors from a set of measurements such that the sources of the observed data are maximally independent [Calhoun and Adali, 2006; Calhoun et al., 2001a, 2002b, 2009; Lange et al., 1999; McKeown et al., 2003, 1998a,b], and thus may help identify neural networks that elude general linear modeling. Briefly, ICA assumes that fMRI signal from each voxel represents a linear mixture of source signals, separates this mixture into spatially independent source signals using higher-order statistics, and groups all brain regions showing synchronized source signals into independent components (ICs) [Calhoun et al., 2002a, 2009; McKeown et al., 1998a; McKeown and Sejnowski, 1998]. Therefore, all voxels/brain regions associated with an IC can be treated as an intrinsically coherent functional network with a unique time course. Brain regions generating more than one source signal may associate with more than one IC with different time courses, and thus two or more ICs may overlap in these brain regions.

As described in detail in our earlier work, ICA may identify networks of brain regions that, because of different or opposite modulation of overlapping voxels, do not manifest significant "activations" to the same events in a GLM [Xu et al., 2015]. For example, we applied ICA to fMRI data collected of a visual task with parametric loads of attention and working memory [Xu et al., 2013]. ICA identified a total of 14 functional networks, which showed different extents of overlap in a majority of brain regions exhibiting any functional activity. Importantly, overlapping functional networks exhibited concurrent but different task-related modulations of time courses. Such task-related, concurrent, but opposite changes in time courses in the same brain regions may not be detected by analyses based on GLM. Thus, multiple cognitive processes may engage common brain regions and exhibit simultaneous but different modulations in time courses during cognitive tasks. These functional networks may be revealed with ICA.

In our earlier work, we used ICA to identify networks of brain regions and characterized how different events—G, SS, and SE—partake in these functional networks [Zhang and Li, 2012]. We characterized six independent components (ICs), including a motor cortical network for motor preparation and execution, a right fronto-parietal network for attentional monitoring, a left fronto-parietal network for response inhibition, a midline cortico-subcortical network for error processing, a cuneus–precuneus network for behavioral engagement, and a "default" network for self-referential processing. However, none of

these ICs demonstrated a correlation with SSRT, which represents the time it requires for the stop process to complete—a key outcome measure of SST. This "negative" finding may reflect a delicate relationship between the activity of ICs and behavioral outcomes, which requires a larger sample size to determine.

Here, we revisited this issue by expanding our sample size to 100 healthy adults and exploring for correlation of the individual beta weights of 23 ICs to SSRT. Our aims are to establish the roles of the neural networks in motor inhibition during cognitive control and to illustrate the broader utility of this data driven method in imaging data analyses.

MATERIALS AND METHODS

Subjects and Behavioral Tasks

One hundred adult healthy subjects (55 males, 27–67 years of age, all right-handed and using their right hand to respond) participated in this study [Hu et al., 2014a]. All subjects were without medical, neurological, and psychiatric illnesses and denied use of illicit substances. All subjects signed a written consent after details of the study were explained, in accordance to institute guidelines and procedures approved by the Yale Human Investigation Committee.

We employed a simple reaction time (RT) task in this stop-signal paradigm, as described in details in our previous studies [Farr et al., 2012; Hendrick et al., 2010; Li et al., 2005; Li et al., 2006; Zhang and Li, 2012]. Briefly, there were two trial types: "go" and "stop," randomly intermixed in presentation. A small dot appeared on the screen to engage attention at the beginning of a go trial. After a randomized time interval (fore-period) anywhere between 1 and 5 s, the dot turned into a circle, prompting the subjects to quickly press a button. The circle vanished at button press or after 1 s had elapsed, whichever came first, and the trial terminated. A premature button press prior to the appearance of the circle also terminated the trial. Approximately three quarters of all trials were go trials. In a stop trial, an additional "X," the "stop" signal, appeared after the go signal following a stop signal delay (SSD). The subjects were told to withhold button press upon seeing the stop signal. Likewise, a trial terminated at button press or when 1 s had elapsed since the appearance of the stop signal. The stop trials constituted approximately one quarter of the trials. There was an inter-trial-interval of 2 s. The SSD started at 200 ms and varied from one stop trial to the next according to a staircase procedure, each increasing and decreasing by 64 ms following a SS and SE trial [De Jong et al., 1990; Levitt, 1971]. With the staircase procedure, a "critical" SSD could be computed that represents the time delay required for the subject to succeed in withholding a response half of the stop trials [Levitt, 1971]. Subjects were instructed to respond to the go signal quickly while keeping in mind that a stop signal could come up in a small number of trials. Each subject completed four 10-min runs of the task. Depending on the actual stimulus timing (e.g., trials varied in foreperiod duration) and speed of response, the total number of trials varied slightly across subjects in an experiment. With the staircase procedure we anticipated that the subjects would succeed in withholding their response in ~50% of the stop trials.

Analyses of Behavioral Data

We computed a critical SSD that represents the time delay between go and stop signals that a subject would need to succeed in 50% of the stop trials [Levitt, 1971]. Specifically, SSDs across trials were grouped into runs, with each run defined as a monotonically increasing or decreasing series. We derived a mid-run estimate by taking the middle SSD (or average of the two middle SSDs when there was an even number of SSDs) of every second run. The critical SSD was computed by taking the mean of all mid-run SSDs. It was reported that, except for experiments with a small number of trials (less than 30), the mid-run estimate was close to the maximum likelihood estimate of X_{50} (50% positive response; i.e., 50% SS in the SST [Wetherill et al., 1966]. The SSRT was computed by subtracting the critical SSD from the median go trial RT [Logan, 1994].

Imaging Protocol

Conventional T1-weighted spin echo sagittal anatomical images were acquired for slice localization using a 3 T scanner (Siemens Trio). Anatomical images of the functional slice locations were next obtained with spin echo imaging in the axial plane parallel to the AC–PC line with TR (Repetition Time) = 300 ms, TE (Echo Time) = 2.5 ms, bandwidth = 300 Hz/pixel, flip angle = 60°, field of view = 220 mm × 220 mm, matrix = 256 × 256, 32 slices with slice thickness = 4 mm and no gap. Functional, blood oxygenation-level dependent (BOLD) signals were then acquired with a single-shot gradient echo-planar imaging (EPI) sequence. Thirty-two axial slices parallel to the AC–PC line covering the whole brain were acquired with TR = 2,000 ms, TE = 25 ms, bandwidth = 2004 Hz/pixel, flip angle = 85°, field of view = 220 mm × 220 mm, matrix = 64 × 64, 32 slices with slice thickness = 4 mm and no gap.

Spatial Preprocessing

Data were analyzed with Statistical Parametric Mapping (SPM8, Wellcome Department of Imaging Neuroscience, University College London, UK). Images from the first five TRs at the beginning of each trial were discarded to enable the signal to achieve steady-state equilibrium between RF pulsing and relaxation. Standard image preprocessing was

performed. Images of each individual subject were first realigned (motion corrected) and corrected for slice timing. A mean functional image volume was constructed for each subject per run from the realigned image volumes. These mean images were co-registered with the high resolution structural image and then segmented for normalization with affine registration followed by nonlinear transformation [Ashburner and Friston, 1999; Friston et al., 1995a]. The normalization parameters determined for the structure volume were then applied to the corresponding functional image volumes for each subject. Finally, the images were smoothed with a Gaussian kernel of 8 mm at full width at half maximum.

We distinguished four trial outcomes: go success (G), go error (F), SS, and SE trial [Li et al., 2006; Zhang et al., 2014]. A statistical analytical design was constructed for each individual subject, using the GLM with the onsets of go signal in each of these trial types convolved with a canonical hemodynamic response function (HRF) and with its temporal derivative for entry as regressors in the model [Friston et al., 1995b]. Realignment parameters in all six dimensions were entered in the model. The data were high-pass filtered (1/128 Hz cutoff) to remove low-frequency signal drifts. Serial autocorrelation was corrected by a first-degree autoregressive or AR(1) model. The GLM estimated the component of variance that could be explained by each of the regressors.

Independent Component Analysis and Beta Weight Estimation

Preprocessed time series were analyzed with a group ICA algorithm (GIFT, http://mialab.mrn.org/software/gift, version 2.0e) to identify spatially independent and temporally coherent networks [Calhoun and Adali, 2012; Calhoun et al., 2001b, 2009]. ICA is a data-driven multivariate method that identifies distinct groups of brain regions with the same temporal pattern of hemodynamic signal change. We used standard procedure in GIFT. Briefly, data from all participants were concatenated into a single dataset and reduced using two stages of principal component analysis (PCA) [Calhoun, et al., 2001b] and separated into 30 maximally independent components with an infomax algorithm [Bell and Sejnowski, 1995]. The dimensionality was determined by the modified minimal description length (MDL) criteria as implemented in GIFT [Li et al., 2007]. A time course for each IC and its corresponding spatial map, which represents a real contribution to this component time course, was obtained. This analysis was repeated 20 times using ICASSO to assess the repeatability of ICs [Himberg et al., 2004] (Supporting Information Fig. 1). Finally, component time courses and spatial maps were back reconstructed for each participant [Calhoun et al., 2001b; Erhardt et al., 2011; Meda et al., 2009].

A systematic procedure was used to diagnose artifacts and identify functional networks. We used the probabilistic maps of white matter (WM), cerebrospinal fluid (CSF), and gray matter (GM) in MNI space, as provided with SPM8, as templates, and Multiple Linear Regression (MLR) as implemented in the spatial sorting function of GIFT to compare the spatial pattern of each IC with these templates. This analysis generated three correlation coefficients (r^2) for every IC, one for each template. Any ICs showing a high correlation with CSF or WM and low correlation with GM were labeled as artifacts. The threshold was set at $r^2 > 0.05$ based on previous publications [Kim et al., 2009a,b; Xu et al., 2013]. Six ICs (IC4, 8, 9, 10, 18, 20) were diagnosed as artifacts. IC1 was also labeled as artifact because it showed a very low correlation with GM ($r^2 < 0.001$). These seven ICs were thus excluded from further analysis.

In order to examine the task relevance of each component, a multiple regression was applied between the component time courses and the time course of each of the go success (G), SS, and SE trials as embodied in the GLM, with reference time course (event onsets convolved with the canonical hemodynamic response). Thus, this association estimate—beta weight—which represents the degree of synchrony between the component and reference time courses, indicates the extent of engagement of the network during the task event [Meda et al., 2009]. Positive and negative beta weight each indicates positive and negative correlation with the event. Note that the sign of the beta weight reflects the direction in which each component is temporally associated with the event of interest and whether the brain regions within each component partake in this association by activation or deactivation. However, individual brain regions may be involved in multiple components and contribute to the temporal correlation in opposite directions according to their "owning" components [Xu et al., 2013].

We also computed the event-related averages (Z scores) over a window of 32 s of the component time course. Each event-related average depicts the level of activation for that particular component over the course of a typical hemodynamic response.

Correlation of Component Beta Weight to SSRT

We examined the beta weights of these 23 ICs under conditions of go success (G), SS, SE, and SS minus SE (SS − SE) for correlation with the SSRT across all 100 subjects. The results were evaluated with correction for multiple comparison ($P < 0.05/(23 \times 4)$ or $\sim$0.0005).

RESULTS AND DISCUSSION

Stop Signal Performance

Subjects had a mean go trial success (RT < 1 s) rate of 93.6 ± 6.4% (mean ± SD, across subjects) with a median RT of 618 ± 110 ms. The averaged SS rate was 52.7 ± 3.2%,

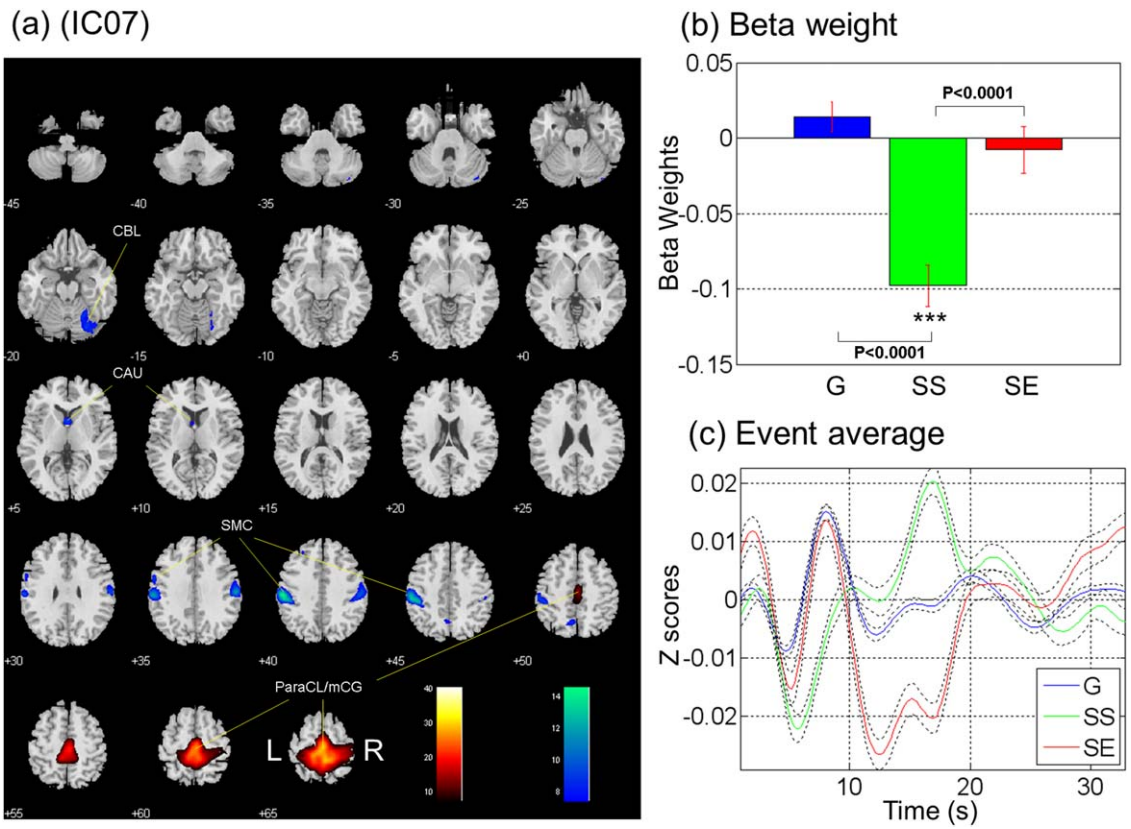

Figure 1.

(a) Paracentral-midcingulate network (IC07); regions with positive and negative signal are identified each by warm and cool colors. (**b**,**c**) Show the beta weights and event averages of G, SS, and SE trials with significant beta weights highlighted: $^{*}P < 0.01$ and $^{***}P < 0.0001$, uncorrected. CBL: cerebellum; CAU: caudate; SMC: sensorimotor cortex; ParaCL/mCG: paracentral lobule/mid-cingulate gyrus. [Color figure can be viewed in the online issue, which is available at wileyonlinelibrary.com.]

suggesting that their performance was adequately tracked by the staircase procedure. The averaged SSRT was 220 ± 44 ms, in the range of the values reported in previous studies [Chang et al., 2015; Farr et al., 2014; Hu et al., 2014a; Hu and Li, 2012; Li et al., 2006 ; Winkler et al., 2013].

Brain Networks of Response Inhibition

After excluding seven artifact ICs, we identified 23 functional networks, each depicting a distinct set of brain regions that show the same pattern of hemodynamic change over time (Supporting Information Figs. 2–4).

In the following, we report the results of correlation across subjects of the beta weight of each of the 23 ICs to SSRT during go success trials (G), SS trials, SE trials, and the contrast SS > SE. Corrected for multiple comparisons by setting an alpha at $0.05/(23 \times 4) = \sim 0.0005$ to guard against type I error, three ICs showed a correlation between SE beta weight and SSRT.

IC07—Paracentral–midcingulate network

The activity (beta weight) of a bilateral (but predominantly right-hemispheric) paracentral–midcingulate cortical network (IC07, Fig. 1) correlated positively with SSRT during SE trials ($P = 0.000016$, $r = 0.42$, Fig. 4a) and negatively with SSRT during SS as compared to SE trials ($P = 0.000031$, $r = -0.40$, Fig. 4d). The beta weight of IC07 did not correlate significantly with SSRT during SS ($P = 0.07$) or G ($P = 0.17$) trial, suggesting that its association with SSRT is mainly driven by activities during SE.

IC07 involves positive modulation of the bilateral and predominantly right-hemispheric paracentral lobules and mid-cingulate cortex, and negative modulation of bilateral (predominantly left-hemispheric) somatomotor cortex and caudate head as well as the right cerebellum. SS showed a significant negative beta weight on IC07 ($t = -7.12$, $P < 0.0001$, one-sample t test). The beta weight on IC07 differs significantly between SS and G ($t = -6.61$, $P < 0.0001$, paired t test) and between SS and SE ($t = -4.38$, $P < 0.0001$, paired t test).

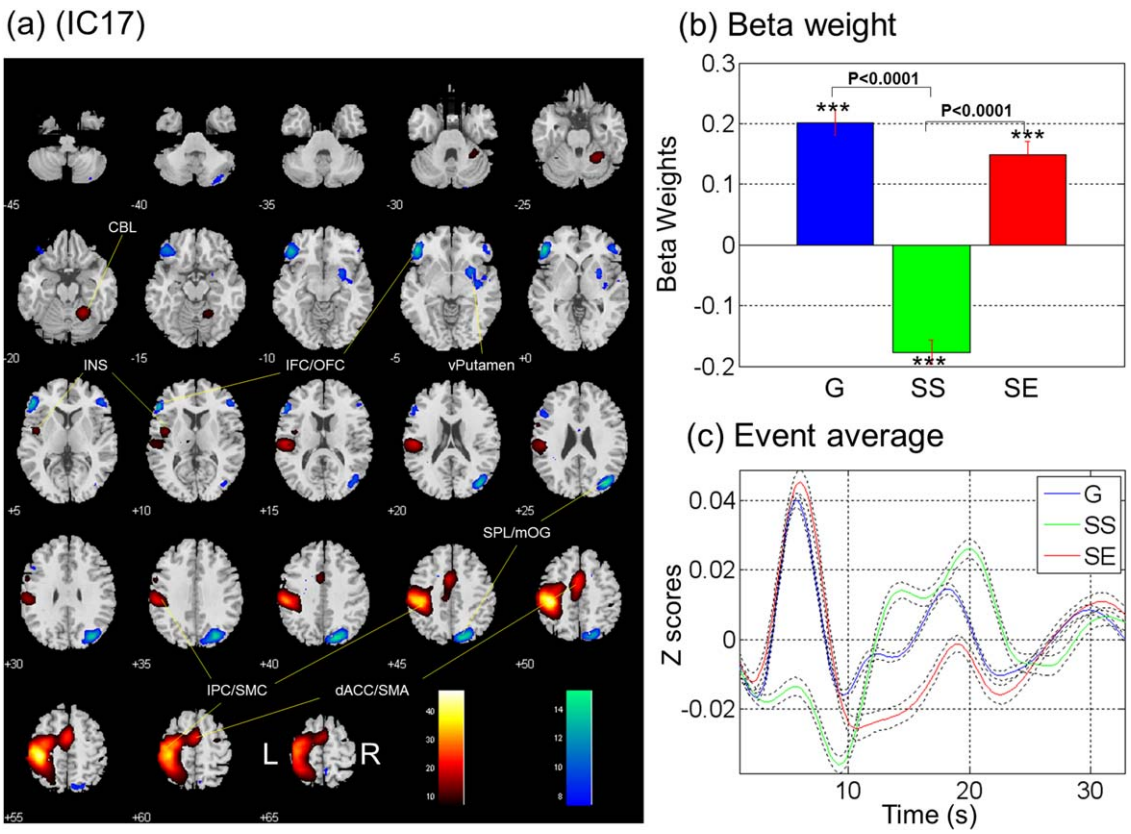

Figure 2.

(a) Left inferior parietal-somatomotor-supplementary motor network (IC17), (**b**) beta weight, and (**c**) event average shown in an identical format. CBL: cerebellum; INS: insula; IFC/OFC: inferior frontal cortex/orbitofrontal cortex; vPutamen: ventral putamen; SPL/mOG: superior parietal lobule/middle occipital gyrus; IPC/SMC: inferior parietal cortex/sensorimotor cortex; dACC/SMA: dorsal anterior cingulate cortex/SMA. [Color figure can be viewed in the online issue, which is available at wileyonlinelibrary.com.]

Thus, activation of bilateral paracentral lobules and mid-cingulate cortex and deactivation of bilateral somatomotor cortices and caudate head as well as the right cerebellum during SE is associated with prolonged SSRT. Both paracentral lobules and mid-cingulate cortex are known to project to downstream motor nuclei, including those in the spinal cord, and respond to movements [Havel et al., 2006; Kishi et al., 2009; Lim et al., 1994; Picard and Strick, 1996; White et al., 1997]. In particular, activation of the mid-cingulate cortex has been associated with the urge to act [Athwal et al., 2001; Farrell et al., 2012; Jackson et al., 2011]. Thus, individuals showing enhanced activity of the paracentral lobules and mid-cingulate cortex are more readily engaged in motor action during SE and prolonged in SSRT. Within IC07, deactivation of bilateral somatomotor cortices during SE is also associated with prolonged SSRT. While contralateral somatomotor cortical activation subserves movement execution, ipsilateral activation is associated with movement suppression as a result of transcortical inhibition [Liang et al., 2014; McGregor et al., in press; Perez et al., 2014; Vidal et al., 2014; Yamanaka et al., 2013]; see also [Cincotta and Ziemann, 2008] for a review. This transcortical inhibition is seen to diminish during aging and certain neurological conditions [Bradnam et al., 2013; Coppi et al., 2014; Rossiter et al., 2014; Sharples et al., 2014; Takechi et al., 2014; Thomalla et al., 2014] known to compromise response inhibition [Hu et al., 2012; Jahanshahi, 2013]. Thus, decreased activation of bilateral somatomotor cortices is consistent with lack of inhibition and prolonged SSRT. The finding of deactivation of the caudate head in link with prolonged SSRT accords with a role of the caudate head in inhibitory control [Boehler et al., 2010; Burke and Barnes, 2011; Hu et al., 2014b; Li et al., 2008c; Padmala and Pessoa, 2010].

IC17—Left inferior parietal–somatomotor–supplementary motor network

Activity of a left inferior parietal–somatomotor–supplementary motor network (IC17, Fig. 2) positively correlated

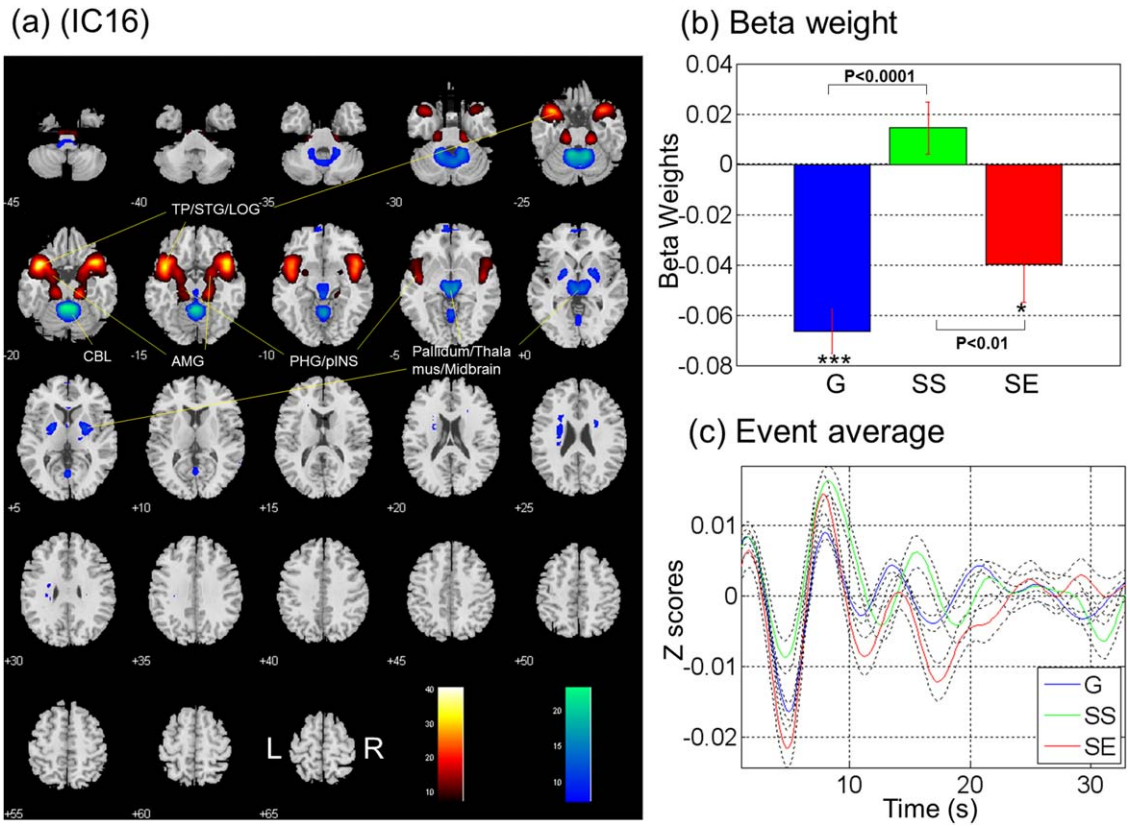

Figure 3.

(a) Pallidal-thalamic/subthalamic-midbrain-midline cerebellar network (IC16), (**b**) beta weight, and (**c**) event average shown in an identical format. TP/STG/LOG: temporal pole/superior temporal gyrus/lateral orbital gyrus; CBL: cerebellum; AMG: amygdala; PHG/pINS: parahippocampal gyrus/posterior insula. [Color figure can be viewed in the online issue, which is available at wileyonlinelibrary.com.]

with SSRT during SE trials ($P = 0.0003$, $r = 0.35$, Fig. 4b) and negatively correlated with SSRT during SS as compared to SE trials ($P = 0.00001$, $r = -0.43$, Fig. 4e). Activity of IC17 did not correlate to SSRT during G ($P = 0.11$) or SS ($P = 0.004$) trial.

IC17 involves positive modulation of the left inferior parietal and somatomotor cortices, SMA, and right cerebellar cortex and negative modulation of the right superior parietal lobule and middle occipital gyrus (SPL/mOG), bilateral but predominantly left inferior frontal cortex and orbitofrontal cortex (IFC/OFC), and right ventral putamen. Both G ($t = 9.52$, $P < 0.0001$, one-sample t test) and SE ($t = 6.89$, $P < 0.0001$, one-sample t test) showed a significantly positive beta weight, while SS ($t = -8.86$, $P < 0.0001$, one-sample t test) showed a significantly negative beta weight, on IC17. The beta weight differed significantly between G and SS as well as between SE and SS ($t = 13.01$ and 11.07; both P's < 0.0001, paired t test).

SE and SS are associated with IC17 each with a positive and negative beta weight, indicating that activation of the left inferior parietal and somatomotor cortex, SMA, and right cerebellar cortex along with deactivation of the left IFC/OFC as well as the right ventral putamen and SPL/mOG expedites motor responses during stop trials.

The contralateral somatomotor cortex and ipsilateral cerebellar cortex responds to the execution of movement [Boscolo Galazzo et al., 2014; Vingerhoets, 2014; Wiese et al., 2004]. Thus, both G and SE load positively on IC17. Deactivation of the right-hemispheric SPL/mOG suggests decreased attentional monitoring for the stop signal [Bartes-Serrallonga et al., 2014; Busan et al., 2009; Capotosto et al., 2013; Coombes et al., 2011; Hillen et al., 2013; Inoue et al., 2000; Li et al., 2006; Lobier et al., 2014; Scheperjans et al., 2005; Vandenberghe and Gillebert 2013; Walz et al., 2014], and SEs result as a consequence. The current finding is also in accord with earlier studies reporting left IFC activation to response inhibition [Goghari and MacDonald, 2009; Rodrigo et al., 2014; Schel et al., 2014; Warren et al., 2013] and deficits in response inhibition as a result of left IFC/OFC damage [Swick et al., 2008]. Activity of right putamen has been associated with short SSRT [Chao et al., 2009; Zandbelt et al., 2013;

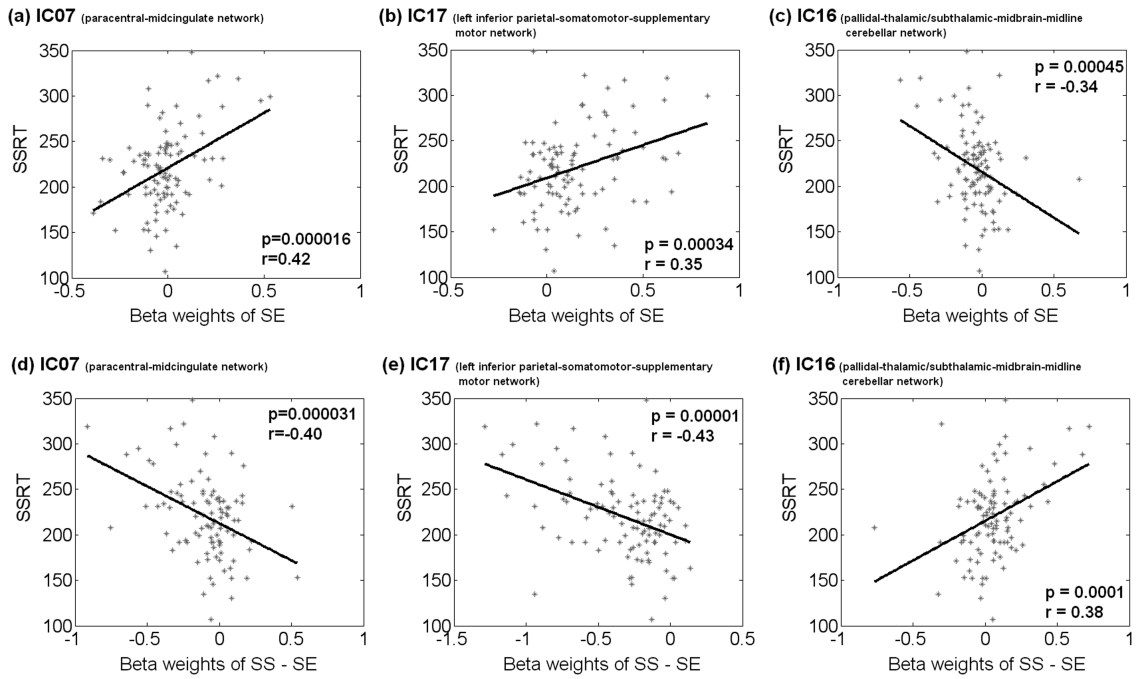

Figure 4.

Simple regression ($n = 100$) showed that activity of the (**a**) paracentral-midcingulate network (IC07) and (**b**) left inferior parietal-somatomotor-supplementary motor network (IC17) correlated positively while activity of the (**c**) pallidal-thalamic/subthalamic-midbrain-midline cerebellar network (IC16) correlated negatively with SSRT during SE trials, and activity of the (**d**) IC07 and (**e**) IC17 correlated negatively while activity of the (**f**) IC16 correlated positively with SSRT during SS as compared to SE trials. Each asterisk represents one subject. These correlations were also confirmed by Spearman regression: there is a positive correlation between SSRT and beta weight of SE for IC07 ($P = 0.0017$, $r = 0.31$) and for IC17 ($P = 0.0016$, $r = 0.31$) as well as between SSRT and beta weight of SS-SE for IC16 ($P = 0.0011$, $r = 0.32$); and a negative correlation between SSRT and beta weight of SE for IC16 ($P = 0.0018$, $r = -0.31$) and beta weight of SS-SE for IC07 ($P = 0.0007$, $r = -0.33$) and for IC17 ($P = 0.0004$, $r = -0.35$).

Zandbelt and Vink, 2010], anti-saccade [Neggers et al., 2012], and proactive inhibition [Vink et al., 2014]. Thus, deactivation of the right putamen relates to SE.

IC16—Pallidal–thalamic/subthalamic–midbrain–midline cerebellar network

Activations of a pallidal–thalamic/subthalamic–midbrain–midline cerebellar network (IC16, Fig. 3) correlated negatively with SSRT during SE ($P = 0.0004$, $r = -0.34$, Fig. 4c) and correlated positively with SSRT during SS > SE ($P = 0.0001$, $r = 0.38$, Fig. 4f). IC16 involves positive modulation of bilateral temporal pole/superior temporal sulcus/lateral orbitofrontal cortex, amygdala, parahippocampal gyrus, and posterior insula, along with negative modulation of the midline cerebellum, pallidum, thalamus, and midbrain. Both G ($t = -7.64$, $P < 0.0001$, one-sample t test) and SE ($t = -2.62$, $P < 0.01$, one-sample t test) are significantly associated with IC16 with a negative beta weight, but not SS ($t = 1.39$, $P = 0.17$, one-sample t test). The beta weight on IC16 also differed significantly between G and SS ($t = -5.97$, $P < 0.0001$, paired sample t test) as well as between SE and SS ($t = -2.95$, $P < 0.01$, paired sample t test).

Thus, deactivation of bilateral temporal pole/superior temporal sulcus/lateral orbitofrontal cortex, amygdala, parahippocampal gyrus, and posterior insula, along with activation of the pallidum, thalamus/subthalamus, midbrain, and midline cerebellum supports movement execution. And the between-subject variation of this activity during SE is positively associated with SSRT. This particular finding is less straightforward to interpret because, firstly, the subnuclei in the pallidum and the subthalamic nucleus appear to play distinct and, in some cases, opposing roles in response execution and inhibition [Isoda and Hikosaka, 2011; Li, 2015]. Secondly, the temporal pole, superior temporal sulcus, lateral orbitofrontal cortex, amygdala, parahippocampal gyrus, or posterior insula are not known for movement control. Rather, the activity of these limbic and paralimbic structures may reflect saliency of the motor response [Litt et al., 2011; Menon and Uddin, 2010; Smith et al., 2011]. For instance, the superior

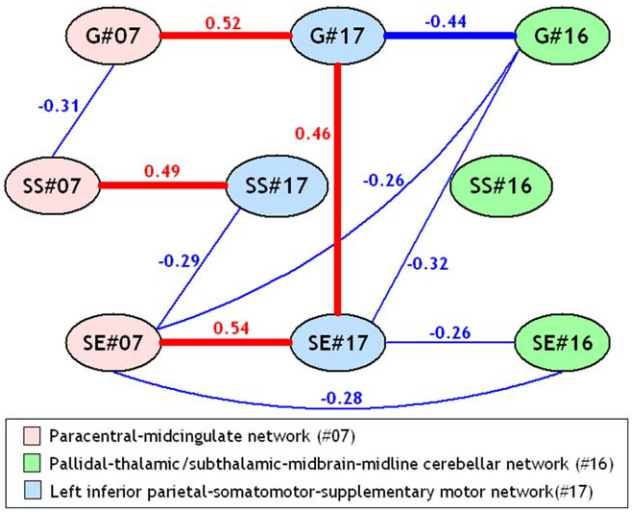

Figure 5.

Pairwise linear regressions across all 100 subjects between beta weights of different components and different trial types. Correlations significant at $P < 0.01$ uncorrected were indicated with lines with bold lines showing those significant at $P < 0.0001$. Red and blue line each indicates a positive and negative correlation. The numbers on the lines are the R values of linear regression. [Color figure can be viewed in the online issue, which is available at wileyonlinelibrary.com.]

temporal cortex and amygdala increased activation to risk taking decisions [Li et al., 2009; Rodrigo et al., 2014]; the lateral orbitofrontal cortex processes implicit motivational value and stimulus saliency [Rothkirch et al., 2012]. Thus, one is tempted to speculate that deactivation of the limbic and paralimbic components of IC16 during SE renders the motor response and error less salient and represents a correlate of prolonged SSRT.

Cross correlation of event beta weights for IC07, IC16, and IC17

We cross-correlated beta weights of IC07, IC16, and IC17 for the same events and between different events for the same component network with pairwise linear regressions. Figure 5 shows those correlations that were significant at an arbitrary threshold of $P < 0.01$, uncorrected, with those significant at $P < 0.0001$ highlighted. A few findings are noteworthy. Examined across the same events, IC17 correlated positively with IC07 ($r = 0.52$, $P < 0.0001$) but negatively with IC16 for G trials ($r = -0.44$, $P < 0.0001$). In addition, IC17 and IC07 but not IC16 correlated also positively for SS ($r = 0.49$, $P < 0.0001$) and SE ($r = 0.54$, $P < 0.0001$) trials. These findings suggest that, while identified as independent networks, both IC07 and IC17 correlated across subjects in beta weights and might serve similar functional roles during the same trial events. In contrast, IC16 correlated negatively with IC17 only during G trials, suggesting that the two networks support opposing patterns of a "default" state of visuomotor response, as go trials dominate the SST.

When examined within the same IC, only IC17 showed a positive correlation in beta weight between G and SE trials, suggesting that IC17 facilitates motor responses; greater activity of IC17 is associated with a decision to respond and minimal attention to the stop signal.

A prediction: Motor urgency and SSRT

Because the correlations we observed with SSRT draw on the SE but not SS trials, it is likely that SSRT is determined primarily by the go process as conceptualized by the interactive race model [Boucher et al., 2007]. That is, an urgency to respond or the extent to which a movement plan is executed interferes with the stop process and prolongs SSRT. In the SST, the reaction time (RT) is shorter in SE than G trials. We posited that the inter-subject variation in how much faster SE trials are, compared to G trials, may reflect motor urgency. To test this hypothesis, we examined whether the RT difference between G and SE, as an index of the extent of movement preparation and execution, is related to the SSRT. Across subjects, both mean RT difference (G – SE) and the effect size of the difference (two-sample t test) showed significant positive correlations with SSRT ($P < 1 \times 10^{-6}$, $r = 0.49$ and $P < 1 \times 10^{-6}$, $r = 0.47$; Fig. 6). Additionally, both mean RT difference and effect size of the difference correlated positively with the activations of IC17 during G ($P = 0.01$, $r = 0.24$ and $P < 0.05$, $r = 0.2$). The mean RT difference also positively correlated with the activation of IC17 during SE ($P = 0.003$, $r = 0.29$). No such correlation was observed for activities in relation to IC07 or IC16. Together, these results support the hypothesis that motor urgency may undermine the stop process and suggest that, of the three components, IC17 perhaps plays the most direct role in determining the SSRT.

GENERAL DISCUSSION

Neural Processes Underlying Stop Errors and SSRT

A most interesting finding concerns the correlation of SE activations with SSRT—activity of IC07 and IC17 are positively correlated, while activity of IC16 is negatively correlated, with SSRT. There are no components with a SS beta weight in correlation with SSRT. This result suggests that regional activations during SEs carry a most significant role in determining the SSRT of individual participants. In contrast, the neural processes of SS do not appear to contribute specifically to SSRT.

It helps explaining this finding by referring to the horse race model of stop signal inhibition, where go and stop processes interact to determine the outcome [Boucher et al., 2007]. Recent studies showed that participants anticipate the stop signal and proactive control determines the

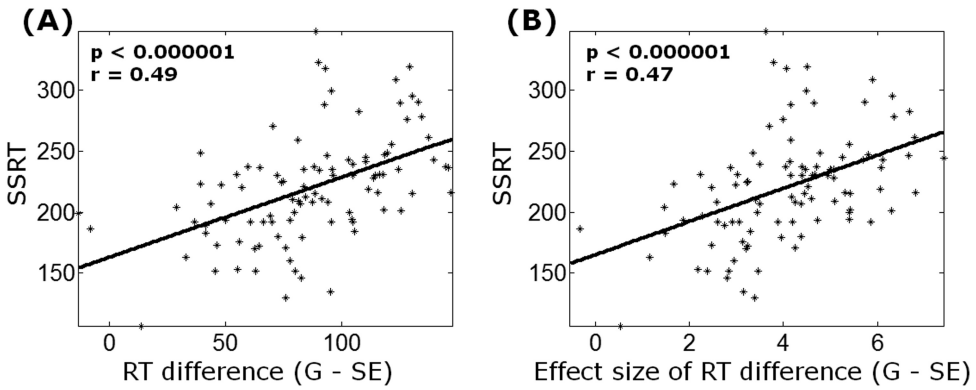

Figure 6.

Across-subject correlation of SSRT and (**a**) the reaction time (RT) difference between G and SE trials; and (**b**) the effect size of RT difference between G and SE trials.

stop trial outcome [Jaffard et al., 2008; Lo et al., 2009; Stuphorn and Emeric, 2012; Vink et al., 2014]. Preparation for motor execution favors a go process and results in SEs. The current findings thus support this thesis by demonstrating that a dominant process of motor execution may impede stop signal inhibition and prolong the SSRT.

In contrast, the lack of significant correlation of any component SS beta weight with SSRT suggests that whatever that takes place during a successful stop trial is not sufficient to determine SSRT. Brain regions such as the inferior frontal and posterior parietal cortex (IC17) contribute to attentional monitoring for the stop signal and successful inhibition but do not influence the SSRT, in accord with our earlier work [Chao et al., 2009; Duann et al., 2009; Li et al., 2006]. It is also worth noting that the components (IC29 and IC30; Supporting Information Fig. 4) comprising the anterior pre-SMA, a structure that has been widely implicated in inhibitory control, does not load on SS with beta weights in correlation with SSRT (both P's > 0.05). This negative finding questions a network role of the pre-SMA in response inhibition, an issue that needs to be further investigated. Together, the current findings emphasize the role of motor activities in determining SSRT, in contrast to a large body of previous work that focused on the "inhibitory" process [Aron, 2007; Band and van Boxtel, 1999; Falkenstein et al., 1999; Huster et al., 2013; Swann et al., 2009; Verbruggen and Logan, 2008].

ICA Versus GLM

We provided the results of linear regression of go and stop events against the SSRT (Supporting Information Methods and Supporting Information Fig. 5). At a threshold of peak voxel $P < 0.001$, uncorrected, there is cluster in the paracentral lobule and posterior/mid-cingulate cortex where activity during SE is positively correlated to SSRT. There were no remarkable findings in the contrast of G or SS events against SSRT. As expected, the regression of SS > SE against SSRT showed that the activity of a similar cluster comprising the paracentral lobule, mid-cingulate gyrus, and left postcentral gyrus in negative correlation with SSRT. Therefore, GLM did reveal cerebral activities that appear to be related to SSRT but not identical to those as described by the ICA. We believe that this discrepancy speaks to the core methodological differences between GLM and ICA and the utility of the ICA in identifying networks of functional significance.

The Relationship Between Contralateral Somatomotor Activity and SSRT Is Component Dependent

The contralateral somatomotor cortex (SMC) showed a pattern of activation that varies with co-occurring activities in its association with SSRT. When contralateral SMC deactivates concurrently with ipsilateral SMC along with activation of the paracentral lobule and the midcingulate cortex, it prolongs SSRT. It also prolongs SSRT when contralateral SMC activates concurrently with the SMA and left inferior parietal cortex along with deactivation of bilateral inferior/orbital frontal cortices and right-hemispheric superior parietal/middle occipital cortices. This component-dependent pattern of activation in a brain region has previously been illustrated in other behavioral tasks and by a direct comparison of findings obtained from GLM and ICA [Domagalik et al., 2012; Kim et al., 2011; Malinen et al., 2007; Tie et al., 2008; Xu et al., 2013]. This finding suggests the complexity of regional cortical activation and cautions the practice of "stand-alone" labeling a brain region in relation to a psychological construct or behavioral performance without considering its interaction with other structures.

CONCLUSIONS

We identified network activities in correlation with SSRT. These findings suggest the utility of ICA in

elucidating a broader network of cerebral activities that synergistically contributes to the efficiency of response inhibition in the SST. The neural mechanisms of motor planning and execution may undercut the stop process and prolongs SSRT.

REFERENCES

Aron AR (2007): The neural basis of inhibition in cognitive control. Neuroscientist 13:214–228.

Ashburner J, Friston KJ (1999): Nonlinear spatial normalization using basis functions. Hum Brain Mapp 7:254–266.

Athwal BS, Berkley KJ, Hussain I, Brennan A, Craggs M, Sakakibara R, Frackowiak RS, Fowler CJ (2001): Brain responses to changes in bladder volume and urge to void in healthy men. Brain 124:369–377.

Band GP, van Boxtel GJ (1999): Inhibitory motor control in stop paradigms: Review and reinterpretation of neural mechanisms. Acta Psychol 101:179–211.

Bartes-Serrallonga M, Adan A, Sole-Casals J, Caldu X, Falcon C, Perez-Pamies M, Bargallo N, Serra-Grabulosa JM (2014): Cerebral networks of sustained attention and working memory: A functional magnetic resonance imaging study based on the continuous performance test. Rev Neurol 58:289–295.

Bell AJ, Sejnowski TJ (1995): An information maximisation approach to blind separation and blind deconvolution. Neural Comput 7:1129–1159.

Boehler CN, Appelbaum LG, Krebs RM, Hopf JM, Woldorff MG (2010): Pinning down response inhibition in the brain—Conjunction analyses of the Stop-signal task. Neuroimage 52:1621–1632.

Boscolo Galazzo I, Storti SF, Formaggio E, Pizzini FB, Fiaschi A, Beltramello A, Bertoldo A, Manganotti P (2014): Investigation of brain hemodynamic changes induced by active and passive movements: A combined arterial spin labeling-BOLD fMRI study. J Magn Reson Imaging 40:937–948.

Boucher L, Palmeri TJ, Logan GD, Schall JD (2007): Inhibitory control in mind and brain: An interactive race model of countermanding saccades. Psychol Rev 114:376–397.

Bradnam LV, Stinear CM, Byblow WD (2013): Ipsilateral motor pathways after stroke: Implications for non-invasive brain stimulation. Front Hum Neurosc 7:184.

Burke MR, Barnes GR (2011): The neural correlates of inhibiting pursuit to smoothly moving targets. J Cogn Neurosci 23:3294–3303.

Busan P, Barbera C, Semenic M, Monti F, Pizzolato G, Pelamatti G, Battaglini PP (2009): Effect of transcranial magnetic stimulation (TMS) on parietal and premotor cortex during planning of reaching movements. PloS One 4:e4621.

Calhoun VD, Adali T (2006): Unmixing fMRI with independent component analysis. IEEE Eng Med Biol Mag 25:79–90.

Calhoun VD, Adali T (2012): Multisubject independent component analysis of fMRI: A decade of intrinsic networks, default mode, and neurodiagnostic discovery. IEEE Rev Biomed Eng 5:60–73.

Calhoun VD, Adali T, McGinty VB, Pekar JJ, Watson TD, Pearlson GD (2001a): fMRI activation in a visual-perception task: Network of areas detected using the general linear model and independent components analysis. Neuroimage 14:1080–1088.

Calhoun VD, Adali T, Pearlson GD, Pekar JJ (2001b): A method for making group inferences from functional MRI data using independent component analysis. Hum Brain Mapp 14:140–151.

Calhoun VD, Adali T, Pearlson GD, van Zijl PC, Pekar JJ (2002a): Independent component analysis of fMRI data in the complex domain. Magn Reson Med 48:180–192.

Calhoun VD, Pekar JJ, McGinty VB, Adali T, Watson TD, Pearlson GD (2002b): Different activation dynamics in multiple neural systems during simulated driving. Hum Brain Mapp 16:158–167.

Calhoun VD, Liu J, Adali T (2009): A review of group ICA for fMRI data and ICA for joint inference of imaging, genetic, and ERP data. Neuroimage 45:S163–S172.

Capotosto P, Tosoni A, Spadone S, Sestieri C, Perrucci MG, Romani GL, Della Penna S, Corbetta M (2013): Anatomical segregation of visual selection mechanisms in human parietal cortex. J Neurosci 33:6225–6229.

Chang A, Chen CC, Li HH, Li CS (2015): Perigenual anterior cingulate event-related potential precedes stop signal errors. Neuroimage 111:179–185.

Chao HH, Luo X, Chang JL, Li CS (2009): Activation of the pre-supplementary motor area but not inferior prefrontal cortex in association with short stop signal reaction time—An intra-subject analysis. BMC Neurosci 10:75.

Cincotta M, Ziemann U (2008): Neurophysiology of unimanual motor control and mirror movements. Clin Neurophysiol 119: 744–762.

Coombes SA, Corcos DM, Vaillancourt DE (2011): Spatiotemporal tuning of brain activity and force performance. Neuroimage 54:2226–2236.

Coppi E, Houdayer E, Chieffo R, Spagnolo F, Inuggi A, Straffi L, Comi G, Leocani L, (2014): Age-related changes in motor cortical representation and interhemispheric interactions: A transcranial magnetic stimulation study. Front Aging Neurosci 6: 209.

De Jong R, Coles MG, Logan GD, Gratton G (1990): In search of the point of no return: The control of response processes. J Exp Psychol Hum Percept Perform 16:164–182.

Domagalik A, Beldzik E, Fafrowicz M, Oginska H, Marek T (2012): Neural networks related to pro-saccades and anti-saccades revealed by independent component analysis. Neuroimage, 62:1325–1333.

Duann JR, Ide JS, Luo X, Li CS (2009): Functional connectivity delineates distinct roles of the inferior frontal cortex and pre-supplementary motor area in stop signal inhibition. J Neurosci 29:10171–10179.

Egner T (2008): Multiple conflict-driven control mechanisms in the human brain. Trends Cogn Sci 12:374–380.

Erhardt EB, Rachakonda S, Bedrick EJ, Allen EA, Adali T, Calhoun VD (2011): Comparison of multi-subject ICA methods for analysis of fMRI data. Hum Brain Mapp 32:2075–2095.

Falkenstein M, Hoormann J, Hohnsbein J (1999): ERP components in go/nogo tasks and their relation to inhibition. Acta Psychol 101:267–291.

Farr OM, Hu S, Matuskey D, Zhang S, Abdelghany O, Li CS (2014): The effects of methylphenidate on cerebral activations to salient stimuli in healthy adults. Experimental and clinical psychopharmacology 22:154–165.

Farr OM, Hu S, Zhang S, Li CS (2012): Decreased saliency processing as a neural measure of Barratt impulsivity in healthy adults. Neuroimage 63:1070–1077.

Farrell MJ, Cole LJ, Chiapoco D, Egan GF, Mazzone SB (2012): Neural correlates coding stimulus level and perception of

capsaicin-evoked urge-to-cough in humans. Neuroimage 61: 1324–1335.

Friston K, Ashburner J, Frith C, Polone J, Heather J, Frackowiak R (1995a): Spatial registration and normalization of images. Hum Brain Mapp 2:165–189.

Friston K, Holmes AP, Worsley KJ, Poline JB, Frith C, Frackowiak R (1995b): Statistical parametric maps in functional imaging: A general linear approach. Hum Brain Mapp 2:189–210.

Friston KJ, Price CJ, Fletcher P, Moore C, Frackowiak RS, Dolan RJ (1996): The trouble with cognitive subtraction. Neuroimage 4:97–104.

Goghari VM, MacDonald AW III (2009): The neural basis of cognitive control: Response selection and inhibition. Brain Cogn 71: 72–83.

Havel P, Braun B, Rau S, Tonn JC, Fesl G, Bruckmann H, Ilmberger J (2006): Reproducibility of activation in four motor paradigms. An fMRI study. J Neurol 253:471–476.

Hendrick OM, Ide JS, Luo X, Li CS (2010): Dissociable processes of cognitive control during error and non-error conflicts: a study of the stop signal task. PloS one 5:e13155.

Hillen R, Gunther T, Kohlen C, Eckers C, van Ermingen-Marbach M, Sass K, Scharke W, Vollmar J, Radach R, Heim S (2013): Identifying brain systems for gaze orienting during reading: fMRI investigation of the landolt paradigm. Front Hum Neurosci 7:384.

Himberg J, Hyvarinen A, Esposito F (2004): Validating the independent components of neuroimaging time series via clustering and visualization. Neuroimage 22:1214–1222.

Hu S, Li CS (2012): Neural processes of preparatory control for stop signal inhibition. Hum Brain Mapp 33:2785–2796.

Hu S, Chao HH, Winkler AD, Li CS (2012): The effects of age on cerebral activations: Internally versus externally driven processes. Front Aging Neurosci 4:4.

Hu S, Chao HH, Zhang S, Ide JS, Li CS (2014a): Changes in cerebral morphometry and amplitude of low-frequency fluctuations of BOLD signals during healthy aging: Correlation with inhibitory control. Brain Struct Funct 219:983–994.

Hu S, Tseng YC, Winkler AD, Li CS (2014b): Neural bases of individual variation in decision time. Hum Brain Mapp 35:2531–2542.

Huster RJ, Enriquez-Geppert S, Lavallee CF, Falkenstein M, Herrmann CS (2013): Electroencephalography of response inhibition tasks: Functional networks and cognitive contributions. Int J Psychophysiol 87:217–233.

Ide JS, Li CS (2011): A cerebellar thalamic cortical circuit for error-related cognitive control. Neuroimage 54:455–464.

Inoue K, Kawashima R, Satoh K, Kinomura S, Sugiura M, Goto R, Ito M, Fukuda H (2000): A PET study of visuomotor learning under optical rotation. Neuroimage 11:505–516.

Isoda M, Hikosaka O (2011): Cortico-basal ganglia mechanisms for overcoming innate, habitual and motivational behaviors. Eur J Neurosci 33:2058–2069.

Jackson SR, Parkinson A, Kim SY, Schuermann M, Eickhoff SB (2011): On the functional anatomy of the urge-for-action. Cogn Neurosci 2:227–243.

Jaffard M, Longcamp M, Velay JL, Anton JL, Roth M, Nazarian B, Boulinguez P (2008): Proactive inhibitory control of movement assessed by event-related fMRI. Neuroimage 42:1196–1206.

Jahanshahi M (2013): Effects of deep brain stimulation of the subthalamic nucleus on inhibitory and executive control over prepotent responses in Parkinson's disease. Front Syst Neurosci 7: 118.

Kim DI, Manoach DS, Mathalon DH, Turner JA, Mannell M, Brown GG, Ford JM, Gollub RL, White T, Wible C, Belger A, Bockholt HJ, Clark VP, Lauriello J, O'Leary D, Mueller BA, Lim KO, Andreasen N, Potkin SG, Calhoun VD (2009a): Dysregulation of working memory and default-mode networks in schizophrenia using independent component analysis, an fBIRN and MCIC study. Hum Brain Mapp 30:3795–3811.

Kim DI, Mathalon DH, Ford JM, Mannell M, Turner JA, Brown GG, Belger A, Gollub R, Lauriello J, Wible C, O'Leary D, Lim K, Toga A, Potkin SG, Birn F, Calhoun VD (2009b): Auditory oddball deficits in schizophrenia: An independent component analysis of the fMRI multisite function BIRN study. Schizophr Bull 35:67–81.

Kim KK, Karunanayaka P, Privitera MD, Holland SK, Szaflarski JP (2011): Semantic association investigated with functional MRI and independent component analysis. Epilepsy Behav 20: 613–622.

Kishi M, Sakakibara R, Nagao T, Terada H, Ogawa E (2009): Thalamic infarction disrupts spinothalamocortical projection to the mid-cingulate cortex and supplementary motor area. J Neurol Sci 281:104–107.

Kok A, Ramautar JR, De Ruiter MB, Band GP, Ridderinkhof KR (2004): ERP components associated with successful and unsuccessful stopping in a stop-signal task. Psychophysiology 41:9–20.

Lange N, Strother SC, Anderson JR, Nielsen FA, Holmes AP, Kolenda T, Savoy R, Hansen LK (1999): Plurality and resemblance in fMRI data analysis. Neuroimage 10:282–303.

Levitt H (1971): Transformed up-down methods in psychoacoustics. J Acoust Soc Am 49 (Suppl 2):467–477.

Li CS, Krystal JH, Mathalon DH (2005): Fore-period effect and stop-signal reaction time. Experimental brain research 167:305–309.

Li CS (2015): Response Inhibition. In: Toga A, editor. Brain Mapping: An Encyclopedia. New York, NY: Elsevier 303–317.

Li CS, Huang C, Constable RT, Sinha R (2006): Imaging response inhibition in a stop-signal task: Neural correlates independent of signal monitoring and post-response processing. J Neurosci 26:186–192.

Li CS, Huang C, Yan P, Paliwal P, Constable RT, Sinha R (2008a): Neural correlates of post-error slowing during a stop signal task: A functional magnetic resonance imaging study. J Cogn Neurosci 20:1021–1029.

Li CS, Yan P, Chao HH, Sinha R, Paliwal P, Constable RT, Zhang S, Lee TW (2008b): Error-specific medial cortical and subcortical activity during the stop signal task: A functional magnetic resonance imaging study. Neuroscience 155:1142–1151.

Li CS, Yan P, Sinha R, Lee TW (2008c): Subcortical processes of motor response inhibition during a stop signal task. Neuroimage 41:1352–1363.

Li CS, Chao HH, Lee TW (2009): Neural correlates of speeded as compared with delayed responses in a stop signal task: An indirect analog of risk taking and association with an anxiety trait. Cereb Cortex 19:839–848.

Li YO, Adali T, Calhoun VD (2007): Estimating the number of independent components for functional magnetic resonance imaging data. Hum Brain Mapp 28:1251–1266.

Liang N, Funase K, Takahashi M, Matsukawa K, Kasai T (2014): Unilateral imagined movement increases interhemispheric inhibition from the contralateral to ipsilateral motor cortex. Exp Brain Res 232:1823–1832.

Lim SH, Dinner DS, Pillay PK, Luders H, Morris HH, Klem G, Wyllie E, Awad IA (1994): Functional anatomy of the human supplementary sensorimotor area: Results of extraoperative electrical stimulation. Electroencephalogr Clin Neurophysiol 91:179–193.

Litt A, Plassmann H, Shiv B, Rangel A (2011): Dissociating valuation and saliency signals during decision-making. Cereb Cortex 21:95–102.

Lo CC, Boucher L, Pare M, Schall JD, Wang XJ (2009): Proactive inhibitory control and attractor dynamics in countermanding action: A spiking neural circuit model. J Neurosci 29:9059–9071.

Lobier MA, Peyrin C, Pichat C, Le Bas JF, Valdois S (2014): Visual processing of multiple elements in the dyslexic brain: Evidence for a superior parietal dysfunction. Front Hum Neurosci 8:479.

Logan GD (1994): On the ability to inhibit thought and action: A users' guide to the stop signal paradigm. In: Dagenbach D, Carr TH, editors. Inhibitory Processes in Attention, Memory and Language. San Diego: Academic Press. pp 189–239.

Logothetis NK (2008): What we can do and what we cannot do with fMRI. Nature 453:869–878.

Malinen S, Hlushchuk Y, Hari R (2007): Towards natural stimulation in fMRI—Issues of data analysis. Neuroimage 35:131–139.

McGregor KM, Sudhyadhom A, Nocera J, Seff A, Crosson B, Butler AJ: Reliability of negative BOLD in ipsilateral sensorimotor areas during unimanual task activity. Brain Imaging Behav (in press).

McKeown MJ, Sejnowski TJ (1998): Independent component analysis of fMRI data: Examining the assumptions. Hum Brain Mapp 6:368–372.

McKeown MJ, Makeig S, Brown GG, Jung TP, Kindermann SS, Bell AJ, Sejnowski TJ (1998a): Analysis of fMRI data by blind separation into independent spatial components. Hum Brain Mapp 6:160–188.

McKeown MJ, Jung TP, Makeig S, Brown G, Kindermann SS, Lee TW, Sejnowski TJ (1998b): Spatially independent activity patterns in functional MRI data during the stroop color-naming task. Proc Natl Acad Sci USA 95:803–810.

McKeown MJ, Hansen LK, Sejnowsk TJ (2003): Independent component analysis of functional MRI: What is signal and what is noise? Curr Opin Neurobiol 13:620–629.

Meda SA, Stevens MC, Folley BS, Calhoun VD, Pearlson GD (2009): Evidence for anomalous network connectivity during working memory encoding in schizophrenia: An ICA based analysis. PloS One 4:e7911.

Menon V, Uddin LQ (2010): Saliency, switching, attention and control: A network model of insula function. Brain Struct Funct 214:655–667.

Neggers SF, Diepen RM, Zandbelt BB, Vink M, Mandl RC, Gutteling TP (2012): A functional and structural investigation of the human fronto-basal volitional saccade network. PloS One 7:e29517.

Padmala S, Pessoa L (2010): Moment-to-moment fluctuations in fMRI amplitude and interregion coupling are predictive of inhibitory performance. Cogn Affect Behav Neurosci 10:279–297.

Perez MA, Butler JE, Taylor JL (2014): Modulation of transcallosal inhibition by bilateral activation of agonist and antagonist proximal arm muscles. J Neurophysiol 111:405–414.

Picard N, Strick PL (1996): Motor areas of the medial wall: A review of their location and functional activation. Cereb Cortex 6:342–353.

Rodrigo MJ, Padron I, de Vega M, Ferstl EC (2014): Adolescents' risky decision-making activates neural networks related to social cognition and cognitive control processes. Front Hum Neurosci 8:60.

Rossiter HE, Davis EM, Clark EV, Boudrias MH, Ward NS (2014): Beta oscillations reflect changes in motor cortex inhibition in healthy ageing. Neuroimage 91:360–365.

Rothkirch M, Schmack K, Schlagenhauf F, Sterzer P (2012): Implicit motivational value and salience are processed in distinct areas of orbitofrontal cortex. Neuroimage 62:1717–1725.

Schel MA, Kuhn S, Brass M, Haggard P, Ridderinkhof KR, Crone EA (2014): Neural correlates of intentional and stimulus-driven inhibition: A comparison. Front Hum Neurosci 8:27.

Scheperjans F, Palomero-Gallagher N, Grefkes C, Schleicher A, Zilles K (2005): Transmitter receptors reveal segregation of cortical areas in the human superior parietal cortex: Relations to visual and somatosensory regions. Neuroimage 28:362–379.

Sharples SA, Almeida QJ, Kalmar JM (2014): Cortical mechanisms of mirror activation during maximal and submaximal finger contractions in parkinson's disease. J Parkinson's Dis 4:437–452.

Smith AB, Halari R, Giampetro V, Brammer M, Rubia K (2011): Developmental effects of reward on sustained attention networks. Neuroimage 56:1693–1704.

Stuphorn V, Emeric EE (2012): Proactive and reactive control by the medial frontal cortex. Front Neuroeng 5:9.

Swann N, Tandon N, Canolty R, Ellmore TM, McEvoy LK, Dreyer S, DiSano M, Aron AR (2009): Intracranial EEG reveals a time- and frequency-specific role for the right inferior frontal gyrus and primary motor cortex in stopping initiated responses. J Neurosci 29:12675–12685.

Swann NC, Cai W, Conner CR, Pieters TA, Claffey MP, George JS, Aron AR, Tandon N (2012): Roles for the pre-supplementary motor area and the right inferior frontal gyrus in stopping action: Electrophysiological responses and functional and structural connectivity. Neuroimage 59:2860–2870.

Swick D, Ashley V, Turken AU (2008): Left inferior frontal gyrus is critical for response inhibition. BMC Neurosci 9:102.

Takechi U, Matsunaga K, Nakanishi R, Yamanaga H, Murayama N, Mafune K, Tsuji S (2014): Longitudinal changes of motor cortical excitability and transcallosal inhibition after subcortical stroke. Clin Neurophysiol 125:2055–2069.

Thomalla G, Jonas M, Baumer T, Siebner HR, Biermann-Ruben K, Ganos C, Orth M, Hummel FC, Gerloff C, Muller-Vahl K, Schnitzler A, Munchau A (2014): Costs of control: Decreased motor cortex engagement during a go/NoGo task in Tourette's syndrome. Brain 137:122–136.

Tie Y, Whalen S, Suarez RO, Golby AJ (2008): Group independent component analysis of language fMRI from word generation tasks. Neuroimage 42:1214–1225.

Vandenberghe R, Gillebert CR (2013): Dissociations between spatial-attentional processes within parietal cortex: Insights from hybrid spatial cueing and change detection paradigms. Front Hum Neurosci 7:366.

Verbruggen F, Logan GD (2008): Response inhibition in the stop-signal paradigm. Trends Cogn Sci 12:418–424.

Vidal AC, Banca P, Pascoal AG, Cordeiro G, Sargento-Freitas J, Castelo-Branco M (2014): Modulation of cortical interhemispheric interactions by motor facilitation or restraint. Neural Plast 2014:210396.

Vingerhoets G (2014): Contribution of the posterior parietal cortex in reaching, grasping, and using objects and tools. Front Psychol 5:151.

Vink M, Zandbelt BB, Gladwin T, Hillegers M, Hoogendam JM, van den Wildenberg WP, Du Plessis S, Kahn RS (2014): Frontostriatal activity and connectivity increase during proactive inhibition across adolescence and early adulthood. Hum Brain Mapp 35:4415–4427.

Winkler AD, Hu S, Li CS (2013): The influence of risky and conservative mental sets on cerebral activations of cognitive control. Int J Psychophysiol 87:254–261.

Walz JM, Goldman RI, Carapezza M, Muraskin J, Brown TR, Sajda P (2014): Simultaneous EEG-fMRI reveals a temporal cascade of task-related and default-mode activations during a simple target detection task. Neuroimage 102:229–239.

Warren SL, Crocker LD, Spielberg JM, Engels AS, Banich MT, Sutton BP, Miller GA, Heller W (2013): Cortical organization of inhibition-related functions and modulation by psychopathology. Front Hum Neurosci 7:271.

Wetherill GB, Chen H, Vasudeva RB (1966): Sequential estimation of quantal response curves: A new method of estimation. Biometrika 53:439–454.

White LE, Andrews TJ, Hulette C, Richards A, Groelle M, Paydarfar J, Purves D (1997): Structure of the human sensorimotor system. I. Morphology and cytoarchitecture of the central sulcus. Cereb Cortex 7:18–30.

Wiese H, Stude P, Nebel K, de Greiff A, Forsting M, Diener HC, Keidel M (2004): Movement preparation in self-initiated versus externally triggered movements: An event-related fMRI-study. Neurosci Lett 371:220–225.

Xu J, Zhang S, Calhoun VD, Monterosso J, Li CS, Worhunsky PD, Stevens M, Pearlson GD, Potenza MN (2013): Task-related concurrent but opposite modulations of overlapping functional networks as revealed by spatial ICA. Neuroimage 79:62–71.

Xu J, Calhoun VD, Potenza MN (2015): The absence of task-related increases in BOLD signal does not equate to absence of task-related brain activation. J Neurosci Methods 240:125–127.

Yamanaka K, Kadota H, Nozaki D (2013): Long-latency TMS-evoked potentials during motor execution and inhibition. Front Hum Neurosci 7:751.

Zandbelt BB, Vink M (2010): On the role of the striatum in response inhibition. PloS One 5:e13848.

Zandbelt BB, Bloemendaal M, Hoogendam JM, Kahn RS, Vink M (2013): Transcranial magnetic stimulation and functional MRI reveal cortical and subcortical interactions during stop-signal response inhibition. J Cogn Neurosci 25:157–174.

Zhang S, Li CS (2012): Functional networks for cognitive control in a stop signal task: Independent component analysis. Hum Brain Mapp 33:89–104.

Zhang S, Hu S, Bednarski SR, Erdman E, Li CS (2014): Error-related functional connectivity of the thalamus in cocaine dependence. NeuroImage Clin 4:585–592.